J. LELITO*#, H. KRAWIEC*, V. VIGNAL**, B. GRACZ*, P.L. ŻAK*, M. SZUCKI*

MODELLING AND SIMULATION OF THE MAGNESIUM PRIMARY PHASE CRYSTALLIZATION IN THE AZ91/SiCp COMPOSITE DEPENDENT ON MASS FRACTION OF SiCp

The aim of this work is to develop a numerical model capable of predicting the grain density in the Mg-based matrix phase of an AZ91/SiC composite, as a function of the total mass fraction of the embedded SiC particles. Based on earlier work in a range of alloy systems, we assume an exponential relationship between the grain density and the maximum supercooling during solidification. Analysis of data from cast samples with different thicknesses, and mass fractions of added SiCp, permits conclusions to be drawn on the role of SiCp in increasing grain density. By fitting the data, an empirical nucleation law is derived that can be used in a micro model. Numerical simulation based on the model can predict the grain density of magnesium alloys containing SiC particles, using the mass fraction of the particles as inputs. These predictions are compared with measured data.

Keywords: numerical simulation, AZ91/SiCp composite, micro-model

1. Introduction

Metal matrix composites (MMC) in comparison to metal alloys have better mechanical properties. MMC composites based on magnesium alloys reinforced with silicon carbide particles have low density and high stiffness as well as a favourable strength-to-mass ratio [1-2]. They have found application in the aerospace and automotive industries [1-2].

Grain size significantly affects the mechanical and corrosion properties of castings [3]. The nucleation of crystals during crystallization is a key factor determining the grain size. Softwares available on the market can simulate the nucleation and growth processes of grains during the crystallization of metals and alloys, thus enabling the prediction of the microstructure [4-6]. However, modelling the crystallization of MMC (with the presence of particles reinforcing the matrix) is more complicated [7-10].

The developed mathematical model of the composite crystallization is based on the heterogeneous nucleation, in which the input parameters were obtained by adjusting the maximum supercooling value and the corresponding grain density. Knowledge of equations describing the function of grains density depending on the supercooling is indispensable when numerically modelling the structure of castings. For these reasons, the issue of nucleation is the subject of numerous theoretical and experimental researches. The result of these investigations is different nucleation laws that bind the degree of supercooling with the rate of nucleation or nucleus density [11-15]. For numerical modelling of the crystallization process, the following relationships are most frequently used: Oldfield [11], Greer [12,13], Fras [14] and Maxwell-Hellawell [15]. The parameters in the grain density function are determined empirically for each physical-chemical state of the liquid alloy. These parameters have already been published for the AZ91 / SiC composite in [16,17]. The proposed model can be used to predict grain density in MMC composites with an AZ91 alloy matrix containing different mass fraction of SiC particles.

2. Mathematical model

The model assumes that the heat transfer process plays a major role in heat transport and therefore the temperature field can be described by the Fourier-Kirchhoff equation with the omission of the element responsible for heat transfer by convection:

$$c_V \frac{\partial T}{\partial \tau} = div\left(\lambda \cdot \text{grad} T\right) + L \frac{\partial f_s}{\partial \tau}, \text{ W} \cdot \text{m}^{-3} \quad (1)$$

where: T – temperature, K; τ – time, s; λ – heat transfer coefficient, $\text{W} \cdot \text{m}^{-1} \cdot \text{K}^{-1}$; c_V – volumetric specific heat, $\text{J} \cdot \text{m}^{-3} \cdot \text{K}^{-1}$; L – latent heat, $\text{J} \cdot \text{m}^{-3}$; f_s – solid phase fraction.

The value of f_S is calculated from the number N_{Vi} and radius R_i of the grains at each iteration step:

$$f_S = 1 - \exp\left(-\sum_{i=1}^{n} \frac{4}{3} \pi R_i^3 N_{Vi}\right) \quad (2)$$

where: N_{Vi} – volumetric grain density for i-class, m^{-3}; R_i – the grain radius for i-class, m.

* AGH UNIVERSITY OF SCIENCE AND TECHNOLOGY, FACULTY OF FOUNDRY ENGINEERING, REYMONTA 23 STR., 30-059 KRAKOW, POLAND
** ICB UMR 6303 CNRS - UNIVERSITÉ BOURGOGNE FRANCHE-COMTÉ, DIJON, FRANCE

Corresponding author: lelito@agh.edu.pl

The volumetric grain density existing in equation (2) was determined in reference [14] based on the heterogeneous nucleation process. In this process, nucleation takes place on the nucleant particle with suitable supercooling. According to Greer et al. [12,13], supercooling is inversely proportional to the diameter of the nucleant particle. The number of nucleation events as a function of supercooling also depends on the size distribution of the nucleant particles. It was found [12,13] that the size distribution of nucleant particles is an exponential function for the largest size nucleant particles on which the nucleation process took place. It was noticed [14] that the size distribution of nucleant particles can lead to the Weibull distribution with module one, which leads to a simple exponential distribution. All these distributions resemble the exponential distribution for the largest size nucleant particles.

The equation given by Fras [14] is based on the inverse dependence of the volumetric grains density on the maximum supercooling:

$$N_V = N_p \cdot \exp\left(-\frac{Z}{\Delta T_{\max}}\right), \text{m}^{-3} \qquad (3)$$

where: N_p – total nucleant particle density in liquid, m^{-3}; Z – nucleation coefficient, K.

Using equations (2) and (3), you can calculate the total grain growth rate, which is described by equation (4). The first part of equation (4) corresponds to the growth rate of existing solid phase grains, while the second part of the following equation is associated with the increasing number of solid phase grains.

$$\frac{\partial f_S}{\partial \tau} = (1 - f_S)\left(\sum_{i=1}^{n} 4\pi R_i^2 N_i \frac{\partial R_i}{\partial \tau} + \frac{4}{3}\pi R_{n+1}^3 \frac{\partial N_V}{\partial \tau}\right), \text{s}^{-1} \qquad (4)$$

where: N_i and R_i – the number and radius of the grains at each iteration step.

To calculate the grain growth rate, the above model must be conjugated with diffusion model of the composite crystallization. For this purpose, a model of spherical grain growth was considered, which is controlled by the diffusion of the solute component (in this case by the diffusion of Al in the Mg-based liquid in front of the moving solid-liquid interface). The diffusion of the alloying component runs between the spherical grain and the surrounding liquid within a closed spherical volume with radius $R_{\max}$. The interphase boundary moving between the grain and the liquid can be described by the second Fick's law and the mass balance. In the spherical coordinate system, the transient concentrations of aluminium in the solid and liquid phase are described respectively [18-20]:

- for grain:

$$\frac{dC(r,\tau)}{d\tau} = D_\alpha\left(\frac{\partial^2 C(r,\tau)}{\partial r^2} + \frac{2}{r}\frac{\partial C(r,\tau)}{\partial r}\right) +$$
$$+ \frac{r}{R}\frac{\partial C(r,\tau)}{\partial r}\frac{dR}{d\tau} \qquad (5)$$

- for liquid:

$$\frac{dC(r,\tau)}{d\tau} = D_L\left(\frac{\partial^2 C(r,\tau)}{\partial r^2} + \frac{2}{r}\frac{\partial C(r,\tau)}{\partial r}\right) +$$
$$+ \frac{R_{\max} - r}{R_{\max} - R}\frac{\partial C(r,\tau)}{\partial r}\frac{dR}{d\tau} \qquad (6)$$

where: r – distance from the grain centre, m; C – percent fraction of the Al, wt.%; $R_{\max}$ – the maximum radius of a spherical grain if the remaining liquid solidifies to one single grain, m; D_α, D_L – the diffusion coefficients of the Al in the grain and in the liquid, m$^2 \cdot$s^{-1}.

For the interphase boundary, equations (5) and (6) are conjugated with the mass balance equation. The interphase boundary movement is connected with concentration of gradient of the alloying element both in the grain and in the surrounding liquid.

The mass balance equation at the grain distribution surface – the surrounding liquid, takes the following form:

$$\left(C_L^* - C_S^*\right)\frac{dR}{d\tau} = D_\alpha \left.\frac{dC(r,\tau)}{dr}\right|_{r\to R^-} - D_L \left.\frac{dC(r,\tau)}{dr}\right|_{r\to R^+} \qquad (7)$$

where: C_L^*, C_S^* – the equilibrium concentration of the Al in the liquid and in the grain, respectively, wt.%.

3. Model assumptions

In the model described above, constant values of thermal-physical coefficients were adopted. As a result of this assumption, it was possible to convert equation (1) to the form:

$$\frac{\partial T}{\partial \tau} = a \cdot \nabla^2 T + \frac{q_V}{c_V}, \text{K} \cdot \text{s}^{-1} \qquad (8)$$

where: $a = \dfrac{\lambda}{c_v}$ – thermal diffusivity coefficient, m^{2}s^{-1};

$c_v = c_p \cdot \rho$ – volumetric specific heat, J m^{-3} K^{-1}; c_p – specific heat, J$\cdot$kg^{-1} K^{-1}; ρ – density, kg$\cdot$m^{-3}.

In the case of a cooling process, without heat evolution of crystallization, equation (8) could be described as follows:

$$\frac{\partial T}{\partial \tau} = G, \text{K} \cdot \text{s}^{-1} \qquad (9)$$

where: $G = a \cdot \nabla^2 T$ – cooling rate, K$\cdot$s^{-1}.

The assumption of a constant or temperature-dependent cooling rate, G, allows the micro-macro model to be transformed into a micro model of composite crystallization. This model also takes into account the relationship between the supercooling and grain density for the AZ91/SiCp composite included in the reference [15]. For such conditions it was possible to determine the crystallization kinetics of the casting. Additionally, it was assumed:
a) diffusion coefficients:
$D_\alpha = 2.7 \cdot 10^{-10}$ m^{2}s^{-1}, $D_L = 2.7 \cdot 10^{-8}$ m^{2}s^{-1},

b) nucleation temperature of α-Mg is described by equation (10) (for 5wt.% of SiC$_p$) [16],

$$T_N(mf_{SiC}) = 606 - 5.8 \exp(-90.4\, mf_{SiC}),\ °C \qquad (10)$$

where: mf_{SiC} – mass fraction of SiC particles.

c) pouring temperature is equal to 700°C,

d) grain density function is described by equation (11) (for $d_{SiC} = 45$ μm) [16],

$$N_V\left(\Delta T_{max}, mf_{SiC}\right) = $$
$$= 1.42\cdot 10^{13} \exp\left(61.9\cdot mf_{SiC} - \frac{36.25\cdot \exp\left(29.3\cdot mf_{SiC}\right)}{\Delta T_{max}}\right),\ m^{-3}$$
$$\qquad (11)$$

e) parameter: $L/c_V = 267{,}86$ K [21],

f) assumed the cooling rate, G, depending on the temperature and material of the mould:

$$G(T) = \begin{cases} -40 & \text{for} & T > 625°C \\ \dfrac{200}{T-630} & \text{for}\ 625°C \geq T > 620°C \\ \dfrac{5T - 2900}{T - 630} & \text{for}\ 620°C \geq T > 600°C \\ \dfrac{100}{T - 630} & \text{for} & T \leq 600°C \end{cases},\ K\times s^{-1} \quad (12)$$

4. Results

In order to verify the described model, an experiment was carried out. During this experiment, the thermo-analysis of cooling and solidification process of the AZ91/SiCp composite with 5 wt.% of the silicon carbide particles was perform.

Figure 1 shows the cooling curves of the AZ91 / SiC composite obtained as a result of simulation and experiment. There is a visible consistency of results, especially for the crystallization range of the magnesium primary phase, i.e. in the range from pouring temperat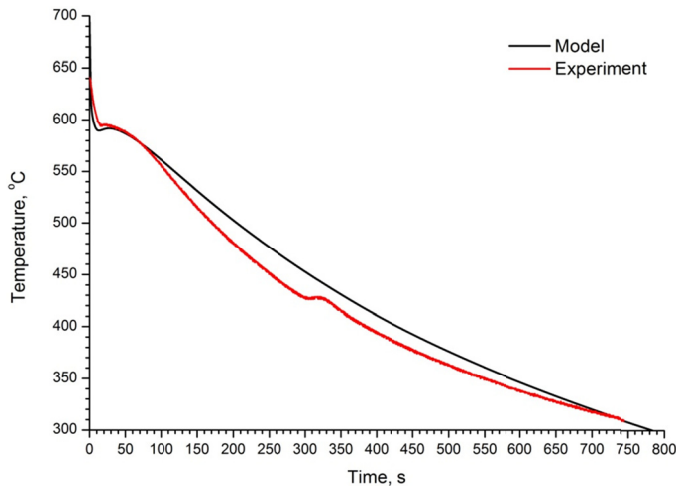ure to 560°C. The eutectic reaction revealed by the thermal arrest at ~460°C on the experimental cooling curve (red colour) was ignored in thy modelling. The differences, in the course of cooling curves, appear only below the temperature of 560°C and may be related to the calculations made for the micro model. In this model, there is no interaction of neighboring numeric grid nodes. The accuracy of the results may also be influenced by the assumption in which the heat dissipation rate does not depend on thermal-physical parameters, but proceeds according to equation (12).

Numerical calculation allows determining the temperature of the end of nucleation process of the α-Mg phase. After this temperature is exceeded, no new grains of the primary phase in the liquid appear, but only their growth. Due to this phenomenon, it is possible to predict the grain density of the α-Mg phase after solidification processes. In the present case, the grain density of the α-Mg phase, obtained as a result of numerical calculations ($N_V = 1.8\cdot 10^{11}$ m^{-3}), is of the same order as the experiment obtained ($N_V = 1.4\cdot 10^{11}$ m^{-3}).

The results of simulation allow to determine the duration of the process of nucleation of the primary phase in the AZ91/5 wt.% SiC, which is equal to 10 s, Fig. 2.

Noteworthy is also the crystallization kinetics of the primary phase, Fig. 3. This graph shows the rapid course of the first
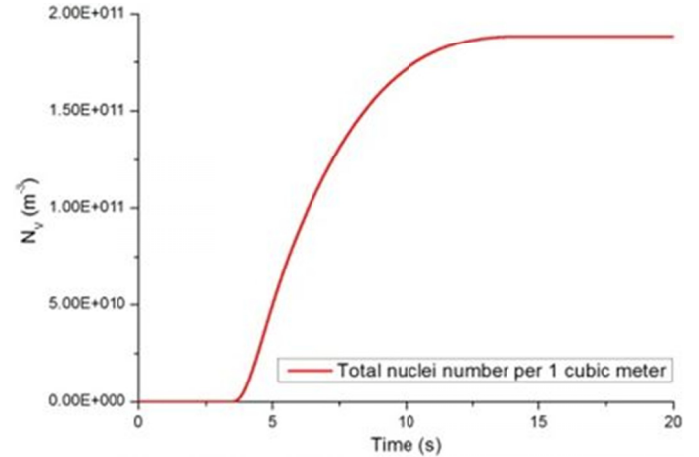

Fig. 2. The nucleation kinetics of the α-Mg primary phase

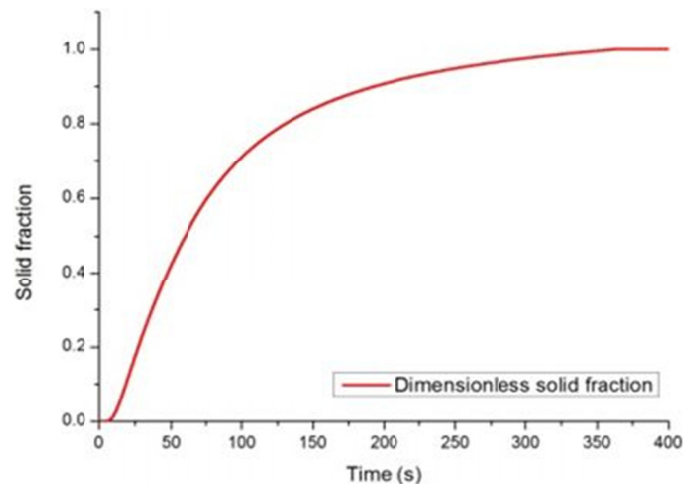Fig. 1. The cooling curves obtained as a result of the simulation and experiment

Fig. 3 The crystallization kinetics of the α-Mg primary phase

crystallization stage, i.e. up to 100 seconds, associated with the growth of the α-Mg grains in the liquid. The second stage, much longer and slower, is associated with the interaction of grains. Growing, in the space depleted in liquid, the grains in contact with each other inhibit their growth.

5. Conclusion

The numerical and experimental experiments of the AZ91/ SiCp crystallization confirm the usefulness of the presented model for grain density prediction in the composite. Compatibility, as to the order of magnitude, of the computed numerical grain density of the α-Mg phase ($N_V = 1.8 \cdot 10^{11}$ m^{-3}) with the density obtained experimentally ($N_V = 1.4 \cdot 10^{11}$ m^{-3}) proves the efficiency of the micro model for simulation the crystallization process of ex-situ composites. Small differences between the results of the numerical and experimental experiment are related to the adopted assumptions.

REFERENCES

[1] L. Drenchev, J. Sobczak, S. Malinov, W. Sha, Model. Simul. Mater. Sci. Eng. **11** (4), 635-649 (2003).

[2] A. Luo, Can. Metall. Quart. **35** (4), 375-383 (1996).

[3] H. Krawiec, J. Lelito, E. Tyrala et al., J. Solid State Electrochem. **13** (6), 935-942 (2009).

[4] D.M. Stefanescu, G. Upadhya et al., Metall. Trans. **21A,** 997-1005 (1990).

[5] J. Liu, R. Elliott. J. Cryst. Growth **191** (1-2), 261-267 (1998).

[6] M. Rappaz, Ch.A. Gandin, Acta Metall. **41** (2), 345-360 (1993).

[7] R. Gunther, Ch. Hartig, R. Bormann. Acta Mater. **54** (20), 5591-5597 (2006).

[8] J. Lelito, J.Sz. Suchy, P. Żak et al., Polish metallurgy 2006-2010 in time of the worldwide economic crisis. Kraków: AKAPIT, 123-143 (2010).

[9] S.K. Jagadeesh, C.S. Ramesh et al., J. Mat. Proc. Tech. **210** (4), 618-623 (2010).

[10] A. Certin, A. Kalkanli, J. Mat. Proc. Tech. **209** (10), 4795-4801 (2009).

[11] W. Oldfield, Trans. ASM **59**, 945-961 (1966).

[12] A.L. Greer, A.M. Bunn, A. Tronche et al., Acta Mater. **48** (11), 2823-2835 (2000).

[13] A.L. Greer, T.E. Quested, Phil. Mag. **86** (24), 3665-3680 (2006).

[14] E. Fraś, K. Wiencek, M. Górny et al., Mat. Sci. Tech. **19**, 1653-1659 (2003).

[15] I. Maxwell, A. Hellawell, Acta Metall. **23** (2), 229-237 (1975).

[16] J. Lelito, P.L. Zak, J.S. Suchy et al., China Foundry **8** (1), 101-106 (2011).

[17] J. Lelito, P.L. Zak, et al., 69th WFC, Hangzhou, China, 16-20 October, (2010).

[18] R.A. Tanzilli, R.W. Heckel, Trans A.I.M.E. **242**, 2312-2321 (1968).

[19] J.M. Vitek, S.A. Vitek, S.A. David, Metall. Mater. Trans. **26A**, 2007-2014 (1995).

[20] T.C. Illingworth, I.O. Golosnoy, J. Comp. Phys. **209** (1), 207-225 (2005).

[21] Built-in material database of MAGMAsoft 4.2 software. Aachen, Germany (2002).